Integrative and Comparative Biology, volume 50, number 5, pp. 756–767
doi:10.1093/icb/icq120

SYMPOSIUM

Cell Lineage and Fate Map of the Primary Somatoblast of the Polychaete Annelid *Capitella teleta*

Néva P. Meyer and Elaine C. Seaver[1]

Kewalo Marine Laboratory, Pacific Biosciences Research Center, University of Hawaii, 41 Ahui Street, Honolulu, HI 96813, USA

From the symposium "Spiralian Development: Conservation and Innovation" presented at the annual meeting of the Society for Integrative and Comparative Biology, January 3–7, 2010, at Seattle, Washington.

[1]E-mail: seaver@hawaii.edu

Synopsis Like most polychaete annelids, *Capitella teleta* (formerly *Capitella* sp. I) exhibits a highly stereotypic program of early development known as spiral cleavage. Animals with spiral cleavage have diverse body plans, and homologous embryonic cells can be readily identified among distantly related animals. Spiralian embryos are particularly amenable to studies of fate-mapping, and larval fates of identified cells are conserved among diverse taxa. One cell of particular importance in spiralian development is 2d, or the primary somatoblast, which generates ectoderm of the body posterior to the prototroch. We are interested in the evolution of the primary somatoblast, and thus far, the 2d sublineage has only been analyzed in a few species. In *Capitella teleta*, 2d generates ectoderm of the segmented trunk and post-segmental pygidium. In this study, development of the 2d lineage was characterized in detail through intracellular injections of DiI, and time-lapse as well as confocal microscopy to analyze cleavage patterns and the fates of larval cells. Analysis of cleavage patterns reveals that the first bilateral division in the 2d sublineage occurs with the division of $2d^{112}$, the same 2d daughter cell that first divides bilaterally in the polychaete *Platynereis dumerilii*. Larval fates of blastomeres $2d^{1}$, $2d^{2}$, $2d^{11}$, $2d^{12}$, $2d^{112}$, $2d^{1121}$, and $2d^{1122}$ were determined. All cells show stereotypic descendant clones that are consistent with segregation within sublineages. In the first few divisions of the 2d sublineage, larval-specific structures (neurotroch and telotroch) and pygidial ectoderm are segregated from segmental ectoderm and ventral nerve cord. The daughters of the first bilateral division, $2d^{1121}$ and $2d^{1122}$, generate the right and left halves of the segmental ectoderm and ventral nerve cord respectively, although the clones are consistently asymmetric across the dorsal midline. The pattern of cleavage divisions and the fates of the 2d daughters in *Capitella teleta* are compared to those in other spiralians with special attention to annelids.

> *Nothing in the development of* Nereis *has excited my interest in a higher degree than the history of the first somatoblast, which undergoes a long series of divisions, continually changing in their character, comparable in regularity and precision with the cleavage of the ovum itself.*
>
> E. B. Wilson, 1892

Introduction

Many animals pass through a series of stereotypic cleavages during their early development. Differences in size, shape, and position of early blastomeres allow identification of individual cells in the early embryo. The Spiralia are a diverse group of animals that share a common stereotypic, holoblastic cleavage program known as spiral cleavage. Animal clades that exhibit spiral cleavage include annelids, mollusks, nemerteans, polyclad flatworms, sipunculans, echiurans, and potentially other marine invertebrate groups. Recent molecular phylogenetic analyses group Spiralia as a monophyletic clade, making spiral cleavage a likely ancestral feature of the Lophotrochozoa (Dunn et al. 2008; Hejnol et al. 2009; Hejnol 2010). Because individual blastomeres can be identified with confidence, homologous embryonic cells can be compared among distantly related taxa with diverse body plans, making the Spiralia an advantageous group for developmental studies of the evolution of animals' body plans.

Advanced Access publication August 19, 2010

The spiral-cleavage program is characterized by a series of divisions in which the cleavage spindles are oriented obliquely with respect to the animal–vegetal axis of the embryo (for review see Henry and Martindale 1999). The first two divisions have cleavage furrows oriented along the animal–vegetal axis and generate the four blastomeres A, B, C, and D (Fig. 1A). In equally cleaving spiralians, these four cells are of the same size, whereas in unequally cleaving embryos, the D blastomere is typically the largest cell. Beginning at the third cell division, the four blastomeres divide obliquely and often asymmetrically to generate a quartet of smaller cells toward the animal pole; these are called micromeres. The larger vegetal cells are known as macromeres. During the birth of the micromeres, the cleavage spindles form at a 45° angle with respect to the animal–vegetal axis of the embryo. In many spiralians, this first division has a clockwise, or dexiotropic, orientation when viewed from the animal pole (Fig. 1A). The macromeres continue to divide asymmetrically and produce additional quartets of micromeres through alternating 45° angles of cleavage spindles oriented clockwise and counter-clockwise (laeotropic) with respect to the animal–vegetal axis.

Within the Spiralia, there is a standard nomenclature to reference individual cells in the embryo (Fig. 1A). Micromeres are identified with a lower case letter of their quadrant of origin, and the corresponding macromeres are identified with capital letters. Designations of the first quartet of micromeres are prefixed by a "1" (1a, 1b, 1c, and 1d), the second quartet of micromeres by a "2" (2a, 2b, 2c, and 2d), and so on. Likewise, once the first-quartet micromeres are born, the macromeres are designated 1A, 1B, 1C, and 1D, and after birth of second-quartet micromeres, the macromeres are designated 2A, 2B, 2C, and 2D. Divisions of the micromeres are also spiral and denoted by a superscript "1" for the animal-most daughter and superscript "2" for the vegetal daughter (Fig. 1A, e.g., $1a^1$ and $1a^2$). Following formation of the fourth quartet of micromeres, the pattern of cell divisions begins to shift from spiral cleavages to bilaterally symmetrical divisions. Bilateral divisions are apparent by the parallel orientation of the cleavage furrow relative to the animal–vegetal axis, and can be the earliest sign of the bilaterally-symmetric body plan of the adult. Bilateral divisions are often first apparent in the embryo in the daughter cells of micromeres 2d and 4d and in many cases produce two equally-sized daughters.

Because of their stereotypic cleavage patterns and the ability to uniquely identify blastomeres, spiralian embryos are particularly amenable to studies of fate-mapping. In addition to a strict pattern of cleavages, larval fates of identified cells are also largely conserved. For example, each of the blastomeres at the four-cell stage (A, B, C, and D) contributes to one of the four body quadrants of the larva. In addition, the larval eyes typically arise from two of the first-quartet micromeres, 1a and 1c. The majority of the adult mesoderm arises from the mesentoblast 4d, a highly conserved spiralian feature. One cell of particular importance is 2d, the primary somatoblast, which generates the majority of the ectoderm of the body posterior to the prototroch, a locomotory band of cilia anterior to the mouth. In annelids, this includes all of the segmented part of the body and the post-segmental pygidium (for review see Henry and Martindale 1999).

In another study, we generated a fate map for the polychaete annelid *Capitella teleta* (N. P. Meyer et al., manuscript in review). *Capitella teleta* was recently described by Blake et al. (2009) and previously known as *Capitella* sp. I. A fate map was generated by individually labeling identified blastomeres through the formation of fourth quartet of micromeres, and the ultimate fates were characterized for larval stages. In *Capitella teleta*, each blastomere gives rise to a predictable set of descendents and shares a number of features characteristic of the typical spiralian fate map.

Here, we extend our fate mapping to characterize the cleavage pattern and fates of the 2d lineage in more detail. 2d generates nearly all of the segmental and pygidial ectoderm. The transition from spiral to bilateral cleavages and the initial segregation of fates was investigated in the 2d sublineage. Specifically, the larval fates of the 2d daughter cells $2d^1$, $2d^2$, $2d^{11}$, $2d^{12}$, $2d^{112}$, $2d^{1121}$, and $2d^{1122}$ were characterized following blastomere microinjection of lineage tracer. We were particularly interested in whether the segmented trunk segregates from the unsegmented posterior pygidium, whether larval and adult structures segregate, and whether bilaterally-symmetric cell divisions correspond with bilaterally-symmetric descendant clones. We compare the complex pattern of cleavage divisions of 2d and its daughters in *Capitella teleta* to that in other spiralians.

Materials and methods

Animal care

Animal maintenance and the collection of embryos were described for *Capitella teleta* by Seaver and

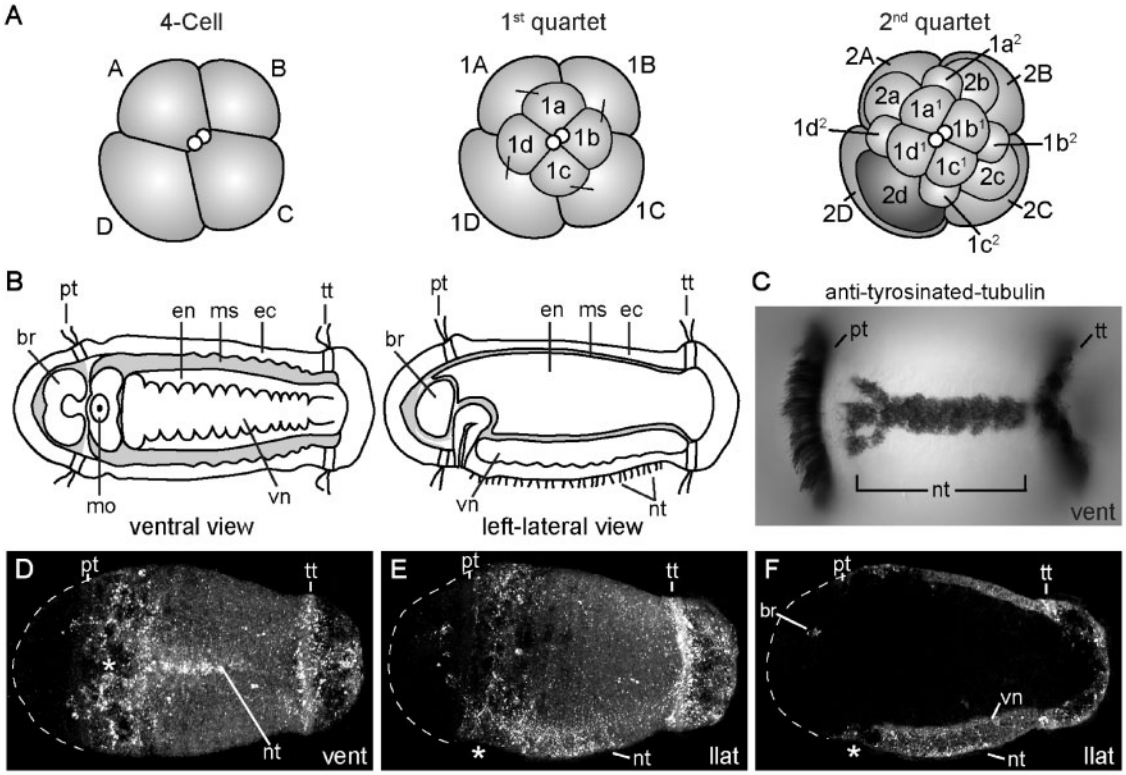

Fig. 1 Development of *Capitella teleta* and contributions of the 2d blastomere to the larval body. (A) Schematic of early cleavages in the *Capitella teleta* embryo. All images are from an animal view. At the four-cell stage, the D blastomere is the largest cell (left panel). The first spiral cleavage occurs at the birth of the first quartet and in *Capitella teleta* is a dexiotropic division (center panel). Right panel shows birth of the second quartet. Note that 2d (dark fill) is the largest cell among the second-quartet micromeres (2a, 2b, 2c, and 2d). (B) Ventral (left panel) and left-lateral (right panel) view schematics of the larval body plan of *Capitella teleta*. (C) Ventral view of a Stage 6 larva labeled with anti-tyrosinated-tubulin showing the position of the ciliary bands of the prototroch (pt), neurotroch (nt), and telotroch (tt). (D–F) Confocal z-stack projections of DiI in late Stage 6 larvae (D, ventral view; E and F, left-lateral views) 5 days after labeling 2d with DiI. An asterisk marks the position of the mouth. Descendants of 2d include the majority of ectoderm posterior to the prototroch, the ventral nerve cord, a few cells in the brain and cells associated with the circumesophageal nerve. Dotted lines mark the anterior edge of the larval head. The confocal z-stack projection in F is centered near the ventral midline and shows DiI labeling that is restricted to the ectoderm, ventral nerve cord and brain. In panels B–F, anterior is to the left. br, brain; ec, ectoderm; en, endoderm; llat, left-lateral; ms, mesoderm; mo, mouth; nt, neurotroch; pt, prototroch; tt, telotroch; vent, ventral; vn, ventral nerve cord.

colleagues (2005). In *Capitella teleta*, embryos are brooded and development is synchronous within a brood. Following injections, animals that were raised to larval stages were kept at 19°C in 0.2 µm filtered sea water (FSW) with 60 µg/mL penicillin and 50 µg/mL streptomycin (Sigma).

DiI labeling of 2d lineage

Prior to injection, the egg shell was permeabilized by a 30 s incubation in a 1:1 mixture of fresh 1 M sucrose and 0.25 M sodium citrate followed by 2–3 FSW rinses. Micromeres were pressure-injected with 1 part $DiIC_{18}(3)$ (1,1′-dioctadecyl-3,3,3′,3′-tetramethylindocarbocyanine perchlorate, Invitrogen) saturated in ethanol to 19 parts soybean oil (Wesson) using aluminosilicate needles (Sutter Instrument Co.). To analyze the division pattern of 2d, 2d-injected embryos were either observed live on a compound microscope or fixed at various cleavage stages according to Meyer and Seaver (2009) (DiI fixation). Fixation times were empirically determined for each experiment by direct observation to optimize fixation times soon after the birth of sequential daughter cells in the 2d sublineage. To analyze the fates of 2d daughters, injected embryos were raised to various larval stages (typically St. 6) and then either imaged live or fixed according to Meyer and Seaver (2009) (DiI fixation). Uninjected and injected animals from a single brood (same stage of development) were raised for the same amount of time, and rates of development and morphological features were compared. At least 90% of the injected plus uninjected animals were healthy for all

experiments (morphologically normal and similar timing of development). Of the $2d^{112}$, $2d^{1121}$, and $2d^{1122}$ injected embryos, 94% (33/35) developed into normal larvae.

For confocal laser scanning microscopy, fixed cleavage-stage embryos and larvae were incubated overnight at 4°C in 1:100 Alexa Fluor 488-phalloidin (Invitrogen) in phosphate-buffered saline (PBS), rinsed 3–4 times in PBS, incubated in SlowFade Gold (Invitrogen) or 80% glycerol in PBS + 0.125 µg/mL Hoechst 33342 (Invitrogen) for at least 3 h at 4°C and then analyzed. Cells were named according to standard spiralian nomenclature (Conklin 1897).

Immunohistochemistry

Fixation of larvae and antibody labeling was performed according to a previously published protocol (Meyer and Seaver 2009). Labeling with 1:5 mouse anti-β-tubulin (E7 supernatant; Developmental Studies Hybridoma Bank developed under the auspices of the NICHD and maintained by The University of Iowa, Department of Biological Sciences, Iowa City, IA, USA) was carried out overnight at 4°C, followed by washes and then incubation with a 1:200 anti-mouse Alexa Fluor 594 secondary antibody for overnight at 4°C. After washing out the secondary antibody, larvae were incubated with a 1:100 dilution of BODIPY FL phallacidin (Invitrogen) for 2 h at RT. Labeling with 1:800 anti-tyrosinated tubulin antibody (TUB-1A2, Sigma) was carried out overnight at 4°C, followed by washes and then a 2 h at RT incubation with 1:300 HRP-conjugated anti-mouse secondary antibody (Jackson ImmunoResearch). HRP labeling was visualized by a colorimetric reaction starting with a 10 min preincubation with 1 mg/mL diaminobenzidene (Sigma) in PBS + 0.1% Triton X-100 (PBT), followed by addition of 0.03% H_2O_2. The reaction was terminated with excess washes of PBT.

Time-lapse video-microscopy and confocal laser scanning microscopy

There were two replicates of the time-lapse movie. For each movie, DiI was injected into the 2d micromere in several embryos. Following each set of injections, a single embryo was mounted with a cover glass on a glass slide in a drop of 0.2 µm FSW surrounded by air and then vacuum grease. The first time-lapse movie (Supplementary Fig. S1) was captured with an Axioskop 2 plus microscope (Zeiss) and an AxioCam HRm camera (Zeiss) using Openlab software version 4.0.1 (Perkin Elmer). Ambient temperature was 20°C. DIC and fluorescent images were manually taken at a single focal plane every 1–20 min for 7 h. The focal plane was adjusted slightly between time points to maintain the 2d clone in focus. The second time-lapse movie was captured with an Axio Imager Z1 microscope (Zeiss) and an ORCA-ER camera (Hamamatsu) using Volocity acquisition software version 5.0 (Perkin Elmer). Ambient temperature was 22°C. DIC and fluorescent z-stacks (5 µm over a 40 µm depth) were automatically taken every 10 min for 8 h.

Confocal laser scanning microscopy was performed using a LSM 510 (for Figs. 1D–F, 3, and 5) and a LSM 710 (for Figs. 2, 4, and 6) confocal microscope (Zeiss). Z-stack projections and movie file were generated using ImageJ (NIH). Figures were constructed using Photoshop CS4 and Illustrator CS4 (Adobe).

Results

Capitella teleta larval body plan and 2d fate

Development of *Capitella teleta* has been previously described and follows a standard staging system (Seaver et al. 2005). Here, we briefly highlight features relevant to this study. Embryos develop by unequal spiral cleavage, allowing individual embryonic quadrants to be identified at the four-cell stage. The D blastomere is the largest cell (Fig. 1A). The first and second-quartet micromeres are born from dexiotropic and laeotropic spiral cleavages, respectively. Cells in the D quadrant divide prior to corresponding cells of the other three quadrants. Thus, 2d is born prior to other second-quartet micromeres. The 2d blastomere is disproportionately large relative to the other second-quartet micromeres and approximates the size of the macromeres, making it readily identifiable (Fig. 1A). Following cleavage and gastrulation, *Capitella teleta* passes through a non-feeding larval stage, which first becomes apparent by formation of the trochal bands after 3 days at 19°C. *Capitella teleta* has multiple larval ciliary bands including a prototroch, telotroch, and neurotroch (Fig. 1B and C). The prototroch is located anterior to the mouth and marks the boundary between the anterior head and segmented trunk. At the posterior end of the trunk, the telotroch marks the boundary between the segmented part of the body and the posterior unsegmented pygidium. The neurotroch is positioned along the ventral midline, extending from the mouth through most of the trunk, with a small gap between its posterior edge and the telotroch. There is also a complex pattern of ciliary bands in the pygidium called the pygidial ciliary band

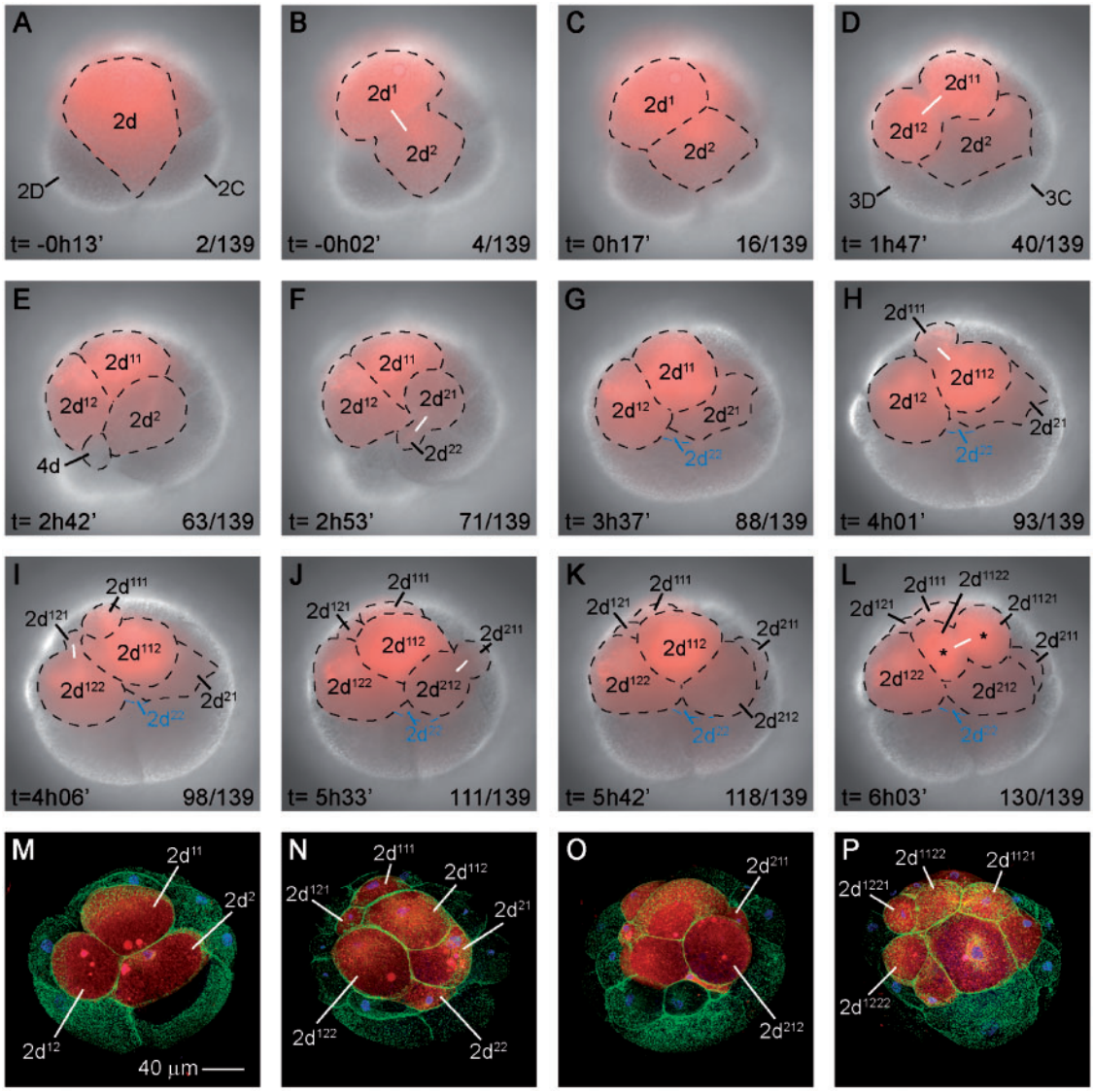

Fig. 2 Cell lineage and cleavage pattern of the primary somatoblast 2d in *Capitella teleta*. (A–L) DiI was microinjected into 2d, and subsequent divisions were followed by time-lapse video microscopy for 7 h at 20°C (Supplementary Fig. 1). Images shown are DIC images overlaid with red fluorescent DiI from the same focal plane. Time points after $2d^1$ is born and movie frame number are shown in the lower-left and -right of each panel, respectively. A white line marks the orientation of cleavage in panels with dividing cells. Cells out of the plane of focus are denoted in blue. 2d daughters and 4d (E) are outlined with dotted lines. Asterisks in L indicate the first bilateral division of the 2d sublineage, the birth of $2d^{1121}$ and $2d^{1122}$. (M–P) Confocal z-stack projections from a side view. Following DiI (red) injection into 2d, embryos were reared for 3–6.5 h at 22°C, fixed, and counterstained with phalloidin (green) to visualize cells' outlines and Hoechst (blue) to visualize nuclei. The scale bar in M is ~40 µm; M–P are to the same scale. All images are from a side view, with the vegetal pole down.

(data not shown) (Eckelbarger and Grassle 1987). During larval development, 13 segments form progressively from anterior to posterior. *Capitella teleta* has a centralized nervous system composed of a brain and a ventral nerve cord with discrete segmental ganglia, which are apparent by mid/late larval stages (Fig. 1B).

Injection of the fluorescent lineage tracer DiI into micromere 2d results in labeling of the majority of ectoderm posterior to the prototroch in larvae (Fig. 1D–F) (N.P. Meyer et al. manuscript in review). This includes the segmented trunk ectoderm, neurotroch, telotroch, and posterior pygidial ectoderm. In addition, 2d generates the ventral nerve cord. 2d also makes a small contribution to the left-dorsal and right-dorsal lobes of the brain and to cells associated with the circumesophageal nerve.

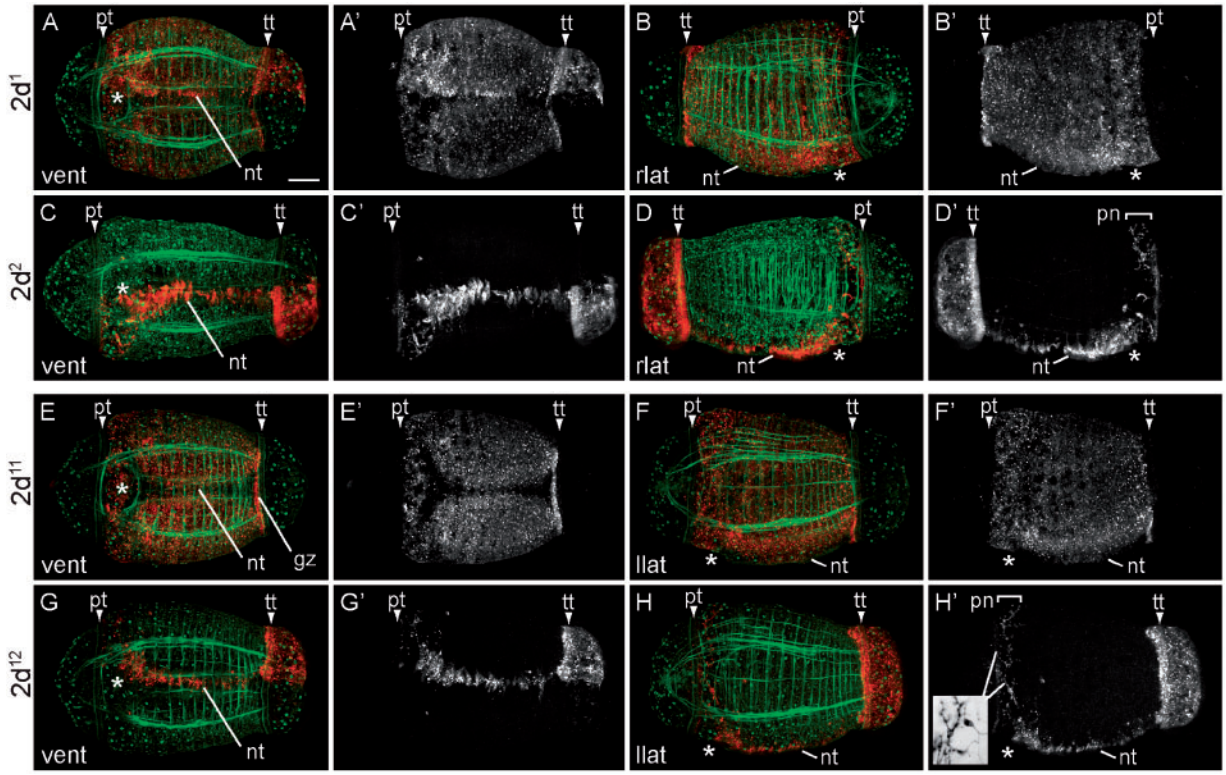

Fig. 3 Daughters of 2d subdivide trunk ectoderm from pygidial ectoderm and trochal bands. (A–H′) Z-stack projections of merged, confocal images of late Stage 6 larvae 5 days after labeling 2d daughters with DiI. The channels are DiI (red) and phalloidin (green). Panels labeled with an apostrophe (e.g. A′) are single-channel images of DiI shown in the panel with the same letter (e.g. A). The position of the ciliary bands of the prototroch (arrowhead, pt), neurotroch (line, nt), and telotroch (arrowhead, tt) are indicated regardless of whether or not the structure is labeled with DiI. In D′ and H′, DiI-labeled peripheral neurons (pn) are indicated by a bracket. Di-labeled ectodermal cells in the posterior growth zone (gz) are indicated in E. The inset in H′ is an inverted, cropped, digital magnification of two DiI-labeled peripheral neurons imaged from a live Stage 6 larva. The approximate position of these neurons is indicated with lines. The micromere labeled with DiI is indicated to the left of each row, while the view is indicated in the lower-left corner of the panel (vent, ventral; llat, left-lateral; and rlat, right-lateral). Anterior is to the left in all ventral and left-lateral images and to the right in all right-lateral images. The scale bar in A is ~40 μm; all images are to approximately the same scale. The position of the mouth is indicated with an asterisk. gz, growth zone; nt, neurotroch; pn, peripheral neurons; pt, prototroch; and tt, telotroch.

Cell division patterns of 2d

DiI was intracellularly microinjected into 2d to analyze the early division patterns of the primary somatoblast (Fig. 2). Divisions were followed directly by time-lapse video microscopy, and by fixing embryos at several intermediate time points for analysis by confocal laser scanning microscopy. In three independent experiments, divisions were followed beginning soon after the birth of 2d until the 2d clone contained 8 cells. In the first experiment conducted at 20°C, a movie was generated from one embryo (Fig. 2A–L, Supplementary Fig. 1). Sixteen additional injected animals from the same brood as the embryo used to generate the first movie were fixed at the following two intermediate times after birth of $2d^1$: 4 h 50 min ($n=6$) and 6 h 30 min ($n=10$). In the second experiment, 2d was injected in 10 embryos and one of these embryos was filmed at 22°C to generate the second movie. Embryos in the third experiment were raised at 22°C, and 28 2d-injected animals from the same brood were fixed at the following six times after birth of $2d^1$: 2 h ($n=4$); 3 h 15 min ($n=4$); 3 h 25 min ($n=4$); 3 h 35 min ($n=4$); 4 h 35 min ($n=6$); and 5 h 10 min ($n=6$). Additional embryos from this brood were raised to Stage 6 larvae and examined for normal development (>90% of injected plus uninjected were normal). The birth of particular cells and the relative order of cell divisions in the 2d sublineage were consistent among both time-lapse movies and the fixed embryos. The exact time between cell divisions was slightly different between the two movies, likely because of differences in the temperature at which the animals were filmed (20 and 22°C) (Table 1). In

addition, there were slight differences in the exact timing of divisions among fixed embryos from the same brood, although these varied within a single cell cycle.

The first division of 2d is dexiotropic, giving rise to $2d^1$ and $2d^2$ (Fig. 2B and C). Prior to additional divisions in the 2d lineage, third-quartet micromeres are born. In the next division, $2d^1$ divides laeotropically to form $2d^{11}$ and $2d^{12}$, such that there are three cells in the 2d sublineage at this stage (Fig. 2D and M). 4d is born (Fig. 2E) prior to the next division, in which $2d^2$ divides laeotropically to produce a smaller vegetal daughter, $2d^{22}$, and a larger animal daughter, $2d^{21}$ (Fig. 2F and G). $2d^{11}$ then divides dexiotropically to generate a smaller animal daughter, $2d^{111}$ and a larger vegetal daughter, $2d^{112}$ (Fig. 2H). This division is immediately followed by a highly asymmetric, dexiotropic division of $2d^{12}$ that produces a smaller animal daughter ($2d^{121}$) and a larger vegetal daughter ($2d^{122}$; Fig. 2I and N). $2d^{21}$ subsequently divides laeotropically to produce a smaller animal daughter ($2d^{211}$) and the larger vegetal daughter ($2d^{212}$; Fig. 2J, K and O). In the next division, $2d^{112}$ divides symmetrically to produce $2d^{1122}$ and $2d^{1121}$ (Fig. 2L and P). This cleavage represents the first bilateral division of the 2d sublineage. The orientation of the cleavage spindle during this division is approximately 90° relative to the animal–vegetal axis, and is different from the orientation of cleavages in the 2d sublineage prior to this division. At this stage the 2d clone contains eight cells. Shortly after cleavage of $2d^{112}$, $2d^{122}$ divides to produce $2d^{1221}$ and $2d^{1222}$ (Fig. 2P).

Fate map of daughters of 2d

The larval fates of the first few divisions of 2d were determined by intracellular labeling of identified blastomeres with DiI, followed by analysis of resulting live and fixed larval stages. The blastomeres examined generate stereotypic descendant clones. The first two divisions of the 2d lineage segregate the neurotroch, telotroch, and pygidial ectoderm from segmented-trunk ectoderm (Figs. 3 and 7). Micromere $2d^2$ generates the right neurotroch, right telotroch, and right pygidial ectoderm ($n = 6$; Fig. 3C–D′). $2d^2$ also forms a few highly-arborized peripheral neurons posterior to the prototroch on the right side of the larva (pn, Fig. 3D and D′, also see inset in Fig. 3H′ for example). Micromere $2d^1$ forms the trunk ectoderm, left neurotroch, left telotroch, and left pygidial ectoderm ($n = 18$; Fig. 3A–B′).

In the next division, $2d^1$ divides to produce the daughter cells $2d^{11}$ and $2d^{12}$. The vegetally-positioned daughter, $2d^{12}$, generates a mirror-image clone of $2d^2$, forming the left neurotroch, left telotroch, left pygidial ectoderm, and some left peripheral neurons ($n = 6$; Fig. 3G–H′). $2d^{11}$ produces the left and right sides of the trunk ectoderm ($n = 15$; Fig. 3E–F′). In addition, descendants of $2d^{11}$ can be seen in the posterior growth zone, visible as a line of labeled cells just anterior to the telotroch on the ventral face of the larva (Fig. 3E, gz). $2d^{11}$ produces the only bilaterally symmetric clone among the cells $2d^1$, $2d^2$, $2d^{11}$, and $2d^{12}$. Interestingly, although they are not sister cells, $2d^2$ and $2d^{12}$ give rise to mirror-image descendant clones, including larval structures (neurotroch and telotroch).

In addition to examining the fates generated by the first few divisions of 2d, we also followed the fates of $2d^{112}$ and its bilateral daughter cells, $2d^{1121}$ and $2d^{1122}$ (Figs. 4, 6 and 7). Injection of DiI into $2d^{112}$ ($n = 11$) generated trunk ectoderm (Fig. 4A–C). In comparison to clones made by the mother cell $2d^{11}$, which give rise to trunk ectoderm extending from the prototroch to the telotroch (Fig. 3E–F′), $2d^{112}$ only generates trunk ectoderm from the mouth to the telotroch, including cells in the posterior growth zone (Fig. 4A–C). In the larvae examined, the region of unlabeled anterior trunk ectoderm extends further posteriorly on the dorsal face relative to the ventral face (Fig. 4A, bracketed region; 4C). This region of anterior trunk ectoderm is presumably generated by $2d^{111}$ (compare Fig. 4C with 3F and F′). Interestingly, when cell outlines are visualized with phallacidin, three distinct regions are apparent within the trunk ectoderm (Fig. 5A). In addition, within the surface ectoderm, there are scattered cells containing actin rings on their apical side that are visible with phalloidin staining and have a

Table 1 Time of blastomere birth for each time-lapse movie. Blastomeres were scored as born once cytokinesis appeared to be complete

	$2d^1$, $2d^2$	$2d^{11}$, $2d^{12}$	$2d^{21}$, $2d^{22}$	$2d^{111}$, $2d^{112}$	$2d^{121}$, $2d^{122}$	$2d^{211}$, $2d^{212}$	$2d^{1121}$, $2d^{1122}$
Movie 1 (20°C)	0h00′	1h50′	3h03′	4h03′	4h09′	5h35′	6h06′
Movie 2 (22°C)	0h00′–0h10′	1h30′–1h40′	2h20′–2h30′	3h20′–3h30′	3h40′–3h50′	4h30′–4h40′	5h00′–5h10′

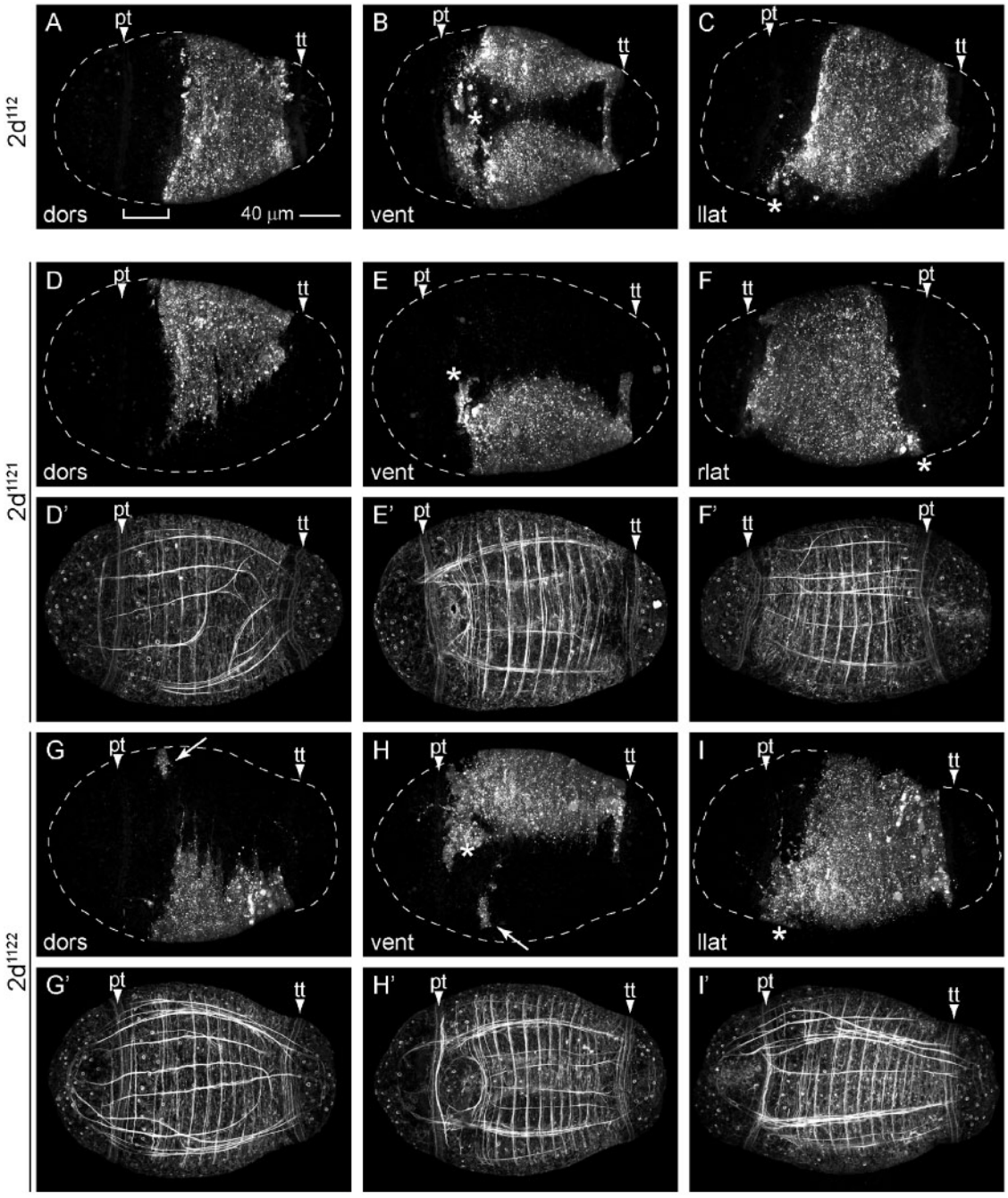

Fig. 4 Fates generated by the first bilateral division of the 2d sublineage. (A–I′) Confocal z-stack projections of Stage 6 larvae 5 days after labeling $2d^{112}$ (A–C), $2d^{1121}$ (D–F′), or $2d^{1122}$ (G–I′) with DiI. The channels are DiI (A–F and G–I), and phalloidin (D′–E′ and G′–I′). Panels labeled with the same letter are from the same z-stack projection. The outline of each larva is shown by a dotted line in the DiI images. The bracket in A denotes the region of unlabeled trunk ectoderm just posterior to the prototroch. The arrows in G and H indicate a band of labeled ectoderm separate from the bulk of the labeled clone. The micromere labeled with DiI is indicated to the left of each row, while the view is indicated in the lower-left corner of the panel (dors, dorsal; llat, left-lateral; rlat, right-lateral; and vent, ventral). Anterior is to the left in all ventral and left-lateral images and to the right in all right-lateral images. The position of the mouth is indicated by an asterisk. The scale bar in A is ~40 μm; all images are to the same scale. pt, prototroch; tt, telotroch.

"s"-shaped morphology (Fig. 3A, C, E, and G). The anterior-most ectodermal region extends from just posterior of the prototroch to posterior of the mouth (Fig. 5A, Region 1). Region 1 has a very different cellular morphology from the middle trunk ectoderm, which is posterior to the mouth (Fig. 5A, Region 2). The anterior boundary of the $2d^{112}$ clones is positioned posterior to this

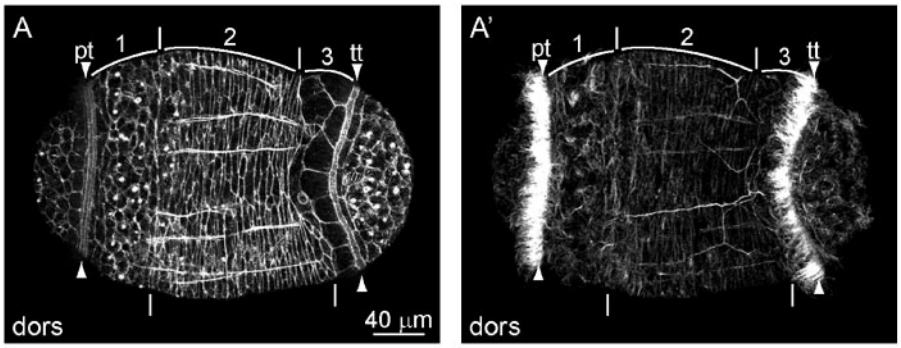

Fig. 5 Organization of the body ectoderm in *Capitella teleta*. (A and A′) Confocal *z*-stack projection through the dorsal surface of a single Stage 6 larva labeled with BODIPY FL phallacidin (A) and anti-β-tubulin (A′). Anterior is to the left. Within the ectoderm of the trunk, three regions of cells with distinct morphologies are visible with phallacidin staining (A). These regions are indicated by horizontal lines and the numbers 1, 2, and 3. The boundaries between these groups of cells are indicated by vertical dashes. Cilia of the prototroch (pt) and telotroch (tt) are visible with anti-β-tubulin labeling (A′). Positions of the prototroch (pt) and telotroch (tt) are indicated by arrowheads. The scale bar is 40 μm. dors, dorsal; pt, prototroch; tt, telotroch.

morphological boundary on the dorsal faces of the larvae. Conversely, on the ventral faces of the larvae, the anterior boundary of the $2d^{112}$ clones is slightly anterior of this morphological boundary (data not shown).

Following the bilateral division of $2d^{112}$, two daughter cells $2d^{1121}$ and $2d^{1122}$ are born. Both cells were individually labeled with DiI and their larval fates analyzed. Micromere $2d^{1121}$ ($n=11$) gives rise to right, trunk ectoderm positioned between the mouth and telotroch, while micromere $2d^{1122}$ ($n=11$) generates left, trunk ectoderm (compare Fig. 4D–F′ with 4G–I′). Clones generated by $2d^{1121}$ and $2d^{1122}$ are largely mirror-images of each other on the ventral and lateral faces of the larvae. Furthermore, the positions of the anterior and ventral boundaries of the descendant clones for both cells have a consistent pattern. However, on the dorsal face of the larvae, $2d^{1121}$ gives rise to a larger area of trunk ectoderm than does $2d^{1122}$ (compare 4D with 4G), and there is some variability in the position of the clonal boundaries on the dorsal face of the descendant clones for both cells; all injected larvae that were scored appeared healthy. For example, the $2d^{1122}$-injected animal in Fig. 4G and H has a band of labeled ectoderm (arrows) on the right side that is positioned apart from the bulk of the clone on the left side. In other $2d^{1122}$-injected animals, this band extended from the bulk of the clone on the left side, across the dorsal face of the larva, terminating anywhere from the dorsal midline to the right ventral face of the larva. The variability in the position of the dorsal edge of the descendant clones of $2d^{1121}$ and $2d^{1122}$ contrasts with the invariant clones generated by the mother of these cells, $2d^{112}$ and with the consistent ventral midline boundary in $2d^{1121}$ and $2d^{1122}$ clones.

In addition to its contribution to trunk ectoderm, $2d^{112}$ generates the ventral nerve cord, and its daughters give rise to the left and right sides of the ventral nerve cord (Fig. 6 and not shown). After injection of $2d^{1122}$, we observed DiI in forming ganglia on the left side of the ventral nerve cord (Fig. 6) and in nerve fibers on the right side of the ventral nerve cord (arrow, Fig. 6B). In conclusion, the first bilateral division of the 2d lineage subdivides the majority of trunk ectoderm and the ventral nerve cord into left and right halves.

Discussion

2d was called the primary somatoblast by early workers in the spiralian field and is generally thought to generate most of the posttrochal ectoderm, or at least to make a disproportionate contribution relative to other second-quartet micromeres. This has been confirmed by modern intracellular fate mapping for the annelids *Helobdella triserialis* (Weisblat et al. 1984), *Tubifex tubifex* (Goto et al. 1999), and *Platynereis dumerilii* (Ackermann et al. 2005), and reported from traditional observations for several other polychaetes including *Amphitrite ornata* (Mead 1894), *Nereis limbata* (Wilson 1892), and *Scoloplos armiger* (Anderson 1959). Our findings that 2d generates almost all the body ectoderm posterior of the prototroch in *Capitella teleta* are consistent with reports for other annelids.

Transition from spiral to bilateral cell divisions

Researchers studying Spiralia have tried to understand how bilaterally symmetric animals arise from

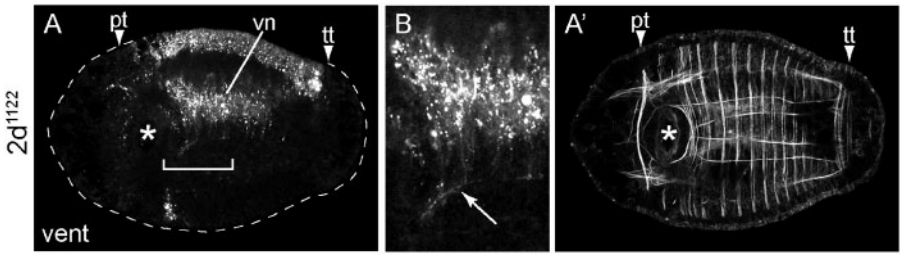

Fig. 6 $2d^{1122}$ generates the left half of the ventral nerve cord in *Capitella teleta*. (A and A′) Confocal z-stack projection through the forming ventral nerve cord in a Stage 6 larva 5 days after labeling $2d^{1122}$. The images are a ventral view with anterior to the left. DiI labeling is shown in A and phalloidin labeling from the same z-stack projection is shown in A′. The position of the mouth is indicated by an asterisk. (B) Cropped, digital magnification (×2.4) of the bracketed region in A. An arrow denotes axons in the ventral nerve cord. pt, prototroch; tt, telotroch; vent, ventral; vn, ventral nerve cord.

a spiral cleavage program. The transition from spiral to bilateral cleavage divisions often initially occurs in the 2d and 4d lineages, and the identity of the cell that undergoes the first bilateral division in these lineages varies among species. In annelids, there appears to be a conservation of when the first bilateral division occurs within the 2d lineage, which occurs at the 4th division cycle of 2d. In the polychaetes *Platynereis dumerilii*, *Platynereis massiliensis*, *Nereis limbata* (Wilson 1892; Dorresteijn 1990; Schneider et al. 1992) and *Capitella teleta* (Fig. 2), the division of $2d^{112}$ to produce $2d^{1121}$ and $2d^{1122}$ is the first bilateral division in the 2d lineage. Furthermore, there is a complex stereotypic pattern of divisions leading to the bilateral division of $2d^{112}$ that is similar among nereid polychaetes and *Capitella teleta* (Wilson 1892; Dorresteijn 1990; Schneider et al. 1992). Specifically, 2d undergoes three spiral cleavages (dexiotropic, Fig. 2B; laeotropic, Fig. 2D; and dexiotropic, Fig. 2H) followed by a fourth cleavage that is bilateral (Fig. 2L). In *Capitella teleta*, the first two spiral cleavages of 2d are nearly equal. The third cleavage is unequal and produces a smaller animal daughter ($2d^{111}$). The fourth division, the bilateral division of $2d^{112}$, is nearly equal. In the leech *Helobdella robusta*, the division pattern of 2d (DNOPQ) differs from that found in polychaetes, although the bilateral division still occurs in the fourth cleavage cycle (Huang et al. 2002). Three smaller animal daughter cells (dnopq′, dnopq″, dnopq‴) are produced by a laeotropic division, a dexiotropic division, and then a division that is parallel to the animal–vegetal axis. In contrast to polychaetes, the first bilateral division in leeches occurs when $2d^{222}$ (DNOPQ‴) divides. This same pattern of 2d divisions has been documented in several clitellates and was likely present in the clitellate ancestor (Dohle 1999). In annelids, the exception to the bilateral division in the sublineage of 2d occurs in the equally cleaving polychaete *Podarke obscura*, in which bilateral divisions of the 2d lineage are not observed (Treadwell 1901).

In mollusks, the large 2d cell in *Unio* exhibits a bilaterally symmetric division in the fifth cleavage cycle, one division later than in *Platynereis dumerilii*, *H. robusta* and *Capitella teleta* (Lillie 1895). In contrast, observations of 2d sublineage divisions past the 4th division cycle in *Crepidula fornicata* reveal only spiral cleavages (Conklin 1897). 2d is similar in size to the other second-quartet micromeres in *Crepidula*, and Conklin argues that the 2d cleavage pattern is more similar to these cells, which is consistent with the fact that 2d does not generate a disproportionate amount of posttrochal ectoderm in this species. In the equally cleaving snail *Limnea stagnalis*, bilateral cleavages begin in the first-quartet micromere $1d^{121}$ (Verdonk 1965). Likewise, in the equally cleaving echiuran *Urechis caupo*, bilateral divisions first occur by meridional cleavages of $1c^{112}$ and $1d^{112}$ (Newby 1932). In the nemertean *Carinoma tremaphoros*, divisions of 2d were followed through the birth of $2d^{11}$, $2d^{12}$, $2d^{21}$, and $2d^{22}$ (Maslakova et al. 2004). Up to this stage, the cleavages of 2d daughters are spiral and unequal, as are the other second-quartet micromeres; thus, additional observations will be necessary to determine if there are bilateral divisions in the 2d lineage of *C. tremaphoros*. In summary, the initiation of bilateral divisions within the 2d sublineage varies among spiralians, is not present in all cases, and may be better correlated with the size of 2d relative to other second-quartet blastomeres rather than with phylogenetic relationships.

Fate map comparisons of the 2d lineage

In *Capitella teleta*, the initial segregation of fates within the 2d sublineage separates the neurotroch, telotroch, and pygidium from the segmental

ectoderm and ventral nerve cord (Fig. 7). The neurotroch and telotroch are larval structures lost at metamorphosis; thus, there is partial segregation of larval structures from adult structures in the trunk ectoderm. It is interesting to note that the mirror-image clones producing larval structures (neurotroch and telotroch) do not arise from sister cells, but rather, are both vegetal daughters ($2d^2$ and $2d^{12}$) of sequential divisions. In addition, in the first two cleavage cycles of 2d, the terminal unsegmented pygidium becomes segregated from the segmented trunk.

The bilateral cell division of $2d^{112}$ in *Capitella teleta* does not correspond with perfectly bilateral descendant clones of the daughter cells $2d^{1121}$ and $2d^{1122}$. Although these cells generate the right and left halves of the segmental ectoderm, respectively, on the dorsal face of the larva, the boundaries of the two clones are not aligned with the midline; the $2d^{1121}$ clone extends well across the midline whereas $2d^{1122}$ does not extend to the midline. Such an asymmetry contrasts with the symmetrical descendant clones of the 2d sublineage in clitellates (Goto et al. 1999; Weisblat et al. 1984) and with the symmetrical descendant clones in the 4d lineage of many spiralians.

With the exception of the clitellate annelids, few modern spiralian fate maps generated using intracellular lineage markers have examined the 2d sublineage in detail. In a 24-h-old *Platynereis dumerilii* larva, descendants of $2d^{112}$ form a bilaterally symmetric clone of dorsal and lateral ectoderm (Ackermann et al. 2005). This differs from $2d^{112}$ descendants in *Capitella teleta*, which form a clone that extends around the circumference of the trunk. This difference may be due to the young age at which the *Platynereis dumerilii* larva was examined, since in *Platynereis*, the ectoderm derived from the D-quadrant moves to a more ventral position at later stages (Wilson 1892; Steinmetz et al. 2007). In the mollusk *Patella vulgata*, a bilaterally symmetric clone forms at an earlier division of the 2d sublineage. Descendants of $2d^1$ and $2d^2$ form mirror-image clones and give rise to the left and right half of the 2d descendant clone, which includes the middle of the foot, the telotroch, the ventral mantle edge, and part of the shell field (Damen 1994).

In clitellate annelids such as *Helobdella triserialis*, *Helobdella robusta*, and *Tubifex tubifex*, the cleavages of 2d that produce the ectodermal teloblasts have been characterized in detail (Weisblat et al. 1984; Goto et al. 1999; Huang et al. 2002). Comparisons with *Capitella teleta* are complicated by the fact that there are several tissues and body domains

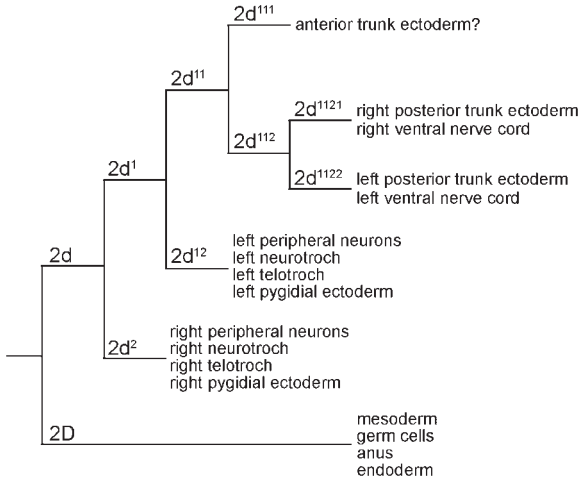

Fig. 7 Diagram showing larval fates generated by daughters of 2d. Fates generated by 2D are described elsewhere (N.P. Meyer et al. in review).

descendant from 2d that are not easily comparable between the two groups of animals. For example, clitellates undergo direct development and do not produce a larval neurotroch or telotroch. Leeches generate a provisional integument not found in *Capitella teleta*, and they do not have postsegmental structures that can be readily homologized to pygidial tissue (the rear sucker is segmental). However, there are some clear differences. At the first division of 2d that generates $2d^1$ and $2d^2$, the origins of the ventral nerve cord and trunk ectoderm segregate differently between *Capitella teleta* and *H. robusta*. In *Capitella teleta*, $2d^1$ generates the ventral nerve cord and segmental ectoderm, whereas in *H. robusta*, descendants of $2d^2$ generate these tissues. If the fates of the cells that undergo the first bilateral division ($2d^{112}$ in *Capitella teleta* and $2d^{222}$ or DNOPQ‴ in *Helobdella robusta*) are compared, both generate the majority of segmental trunk ectoderm and the ventral nerve cord. Furthermore, comparison of the first two cells born in the 2d sublineage that do not contribute to the bilateral division, $2d^2$ and $2d^{12}$ in *Capitella teleta* and $2d^1$ or dnopq′ and $2d^{21}$ or dnopq″ in *H. robusta*, show that both sets of cells generate mirror-image clones that are temporary structures, namely ciliary bands and provisional integument, respectively (Huang et al. 2002). This suggests that the fates of descendant lineages of the first few divisions in the 2d sublineage may have shifted in these two species with respect to each other.

In summary, fates of the 2d sublineage are generally poorly characterized across the Spiralia. We hope that the characterization of the 2d sublineage in *Capitella teleta* will encourage future studies in

other species and contribute to an understanding of the evolution of the primary somatoblast.

Acknowledgment

We acknowledge support from the divisions of Evolutionary Developmental Biology and Developmental and Cell Biology in the Society for Integrative and Comparative Biology.

Funding

The National Science Foundation (IOS09-23754 to E.C.S.).

Supplementary Data

Supplementary Data are available at *ICB* online.

References

Ackermann C, Dorresteijn A, Fischer A. 2005. Clonal domains in postlarval *Platynereis dumerilii* (Annelida: Polychaeta). J Morphol 266:258–80.

Anderson DT. 1959. The embryology of the polychaete *Scoloplos armiger*. Q J Microsc Sci 100:89–166.

Blake JA, Grassle JP, Eckelbarger KJ. 2009. *Capitella teleta*, a new species designation for the opportunistic and experimental *Capitella* sp. I, with a review of the literature for confirmed records. Zoosymposia 2:25–53.

Conklin EG. 1897. The embryology of Crepidula. J Morphol 13:1–226.

Damen P. 1994. Cell-lineage, and specification of developmental fate and dorsoventral organisation in the mollusc *Patella vulgata*. PhD Thesis, University of Utrecht, The Netherlands.

Dohle W. 1999. The ancestral cleavage pattern of the clitellates and its phylogenetic deviations. Hydrobiologia 402:267–83.

Dorresteijn AWC. 1990. Quantitative analysis of cellular differentiation during early embryogenesis of *Platynereis dumerilii*. Roux's Archiv Dev Biol 199:14–30.

Dunn CW, et al. 2008. Broad phylogenomic sampling improves resolution of the animal tree of life. Nature 452:745–9.

Eckelbarger K, Grassle J. 1987. Interspecific variation in genital spine, sperm, and larval morphology in six sibling species of *Capitella*. Bull Biol Soc Wash 7:62–76.

Goto A, Kitamura K, Arai A, Shimizu T. 1999. Cell fate analysis of teloblasts in the Tubifex embryo by intracellular injection of HRP. Dev Growth Differ 41:703–13.

Hejnol A. 2010. A twist in time: the evolution of spiral cleavage in the light of animal phylogeny. Integr Comp Biol published online (doi:10.1093/icb/icq103).

Hejnol A, et al. 2009. Assessing the root of bilaterian animals with scalable phylogenomic methods. Proc Biol Sci 276:4261–70.

Henry JJ, Martindale MQ. 1999. Conservation and innovation in spiralian development. Hydrobiologia 402:255–65.

Huang FZ, Kang D, Ramirez-Weber FA, Bissen ST, Weisblat DA. 2002. Micromere lineages in the glossiphoniid leech *Helobdella*. Development 129:719–32.

Lillie FR. 1895. The embryology of the *Unionidae*. J Morphol 10:1–100.

Maslakova SA, Martindale MQ, Norenburg JL. 2004. Fundamental properties of the spiralian developmental program are displayed by the basal nemertean *Carinoma tremaphoros* (Palaeonemertea, Nemertea). Dev Biol 267:342–60.

Mead AD. 1894. Preliminary account of the cell lineage of *Amphitrite* and other annelids. J Morphol 9:465–73.

Meyer NP, Seaver EC. 2009. Neurogenesis in an annelid: characterization of brain neural precursors in the polychaete *Capitella* sp. I. Dev Biol 335:237–52.

Newby WW. 1932. The early embryology of the echiuroid, *Urechis*. Biol Bull 63:387–99.

Schneider S, Fischer A, Dorresteijn AWC. 1992. A morphometric comparison of dissimilar early development in sibling species of *Platynereis* (Annelida, Polychaeta). Roux's Arch Dev Biol 201:243–56.

Seaver EC, Thamm K, Hill SD. 2005. Growth patterns during segmentation in the two polychaete annelids, *Capitella* sp. I and *Hydroides elegans*: comparisons at distinct life history stages. Evol Dev 7:312–26.

Steinmetz PR, Zelada-Gonzales F, Burgtorf C, Wittbrodt J, Arendt D. 2007. Polychaete trunk neuroectoderm converges and extends by mediolateral cell intercalation. Proc Natl Acad Sci USA 104:2727–32.

Treadwell AI. 1901. Cytology of *Podarke obscura*. J Morphol 17:399–486.

Verdonk NH. 1965. Morphogenesis of the head region in *Limnea stagnalis*. Thesis, University of Utrecht, The Netherlands.

Weisblat DA, Kim SY, Stent GS. 1984. Embryonic origins of cells in the leech *Helobdella triserialis*. Dev Biol 104:65–85.

Wilson EB. 1892. The cell-lineage of *Nereis*. A contribution to the cytogeny of the annelid body. J Morphol 6:361–480.